Modelling of microstructure evolution in advanced high strength steels

M. Militzer, F. Fazeli, H. Azizi-Alizamini

There is currently a significant development of new families of steels, i.e. advanced high strength steels, in response to the demands of the automotive and construction industries for materials with improved property characteristics. The austenite-ferrite transformation is the key metallurgical tool to tailor the properties of steels. The design of processing paths that will lead to the desired microstructures is increasingly been aided by computer simulations. The present paper illustrates state-of-the-art microstructure modelling approaches for low carbon steels considering three important processing aspects: (i) run-out table cooling of hot-rolled steels, (ii) intercritical annealing of cold-rolled sheets, (iii) girth welding of linepipe steels. Phenomenological models based on the Johnson-Mehl-Avrami-Kolmogorov (JMAK) approach incorporating additivity are now available to describe phase transformations during run-out table cooling of microalloyed steels. Strengths and limitations of this approach will be discussed. Process models for intercritical annealing require an accurate description of the austenite formation kinetics where morphological complexities can be captured using the phase field approach. During girth welding the control of the microstructure in the heat affected zone (HAZ) is of paramount importance. The HAZ experiences rapid thermal cycles and steep temperature gradients. Phase field modelling is an excellent tool to describe the role of these spatial constraints as will be illustrated for austenite grain growth.

Keywords: Low carbon steels, Microstructure modelling, Austenite decomposition, Austenite formation, Austenite grain growth, Phase field modelling, Heat affected zone

INTRODUCTION

The development of process models has received significant attention in the steel industry over the past three decades. Starting with the pioneering work of Sellars et al. [1, 2] in the late 1970's mathematical models were in particular developed for hot rolling of steels – initially for plate rolling [3, 4] and subsequently for strip rolling [5, 6, 7, 8, 9]. Today a wealth of sophisticated models is available for most steel processing routes including forging, rod and bar rolling and continuous annealing (and/or hot dip galvanizing) of cold-rolled sheets [10, 11, 12]. There is now also an increasing effort to develop similar models for rapid heat treatment cycles of novel processing routes and those that are typically observed in the HAZ during welding using, for example the approach of Leblond and Devaux [13]. This model development has been made possible by the enormous progress in computer technology over the past decades. Increasingly, many of these models are based on sound physical principles thereby gradually eliminating a number of empirical parameters that need to be determined for each given steel grade with labour intensive experimental laboratory simulations. The availability of such microstructure models is now seen to be of crucial importance to develop new grades and robust processing routes for the production of low carbon sheet steels that are required for some of the most demanding applications of steel, e.g. in the automotive industry and the energy sector. Thus, the present paper provides an overview on state-of-the-art microstructure modelling approaches for these advanced high strength steels with illustrations from three critical processing aspects: (i) run-out table cooling of hot-rolled steels, (ii) intercritical annealing of cold-rolled sheets, (iii) girth welding of linepipe steels.

Matthias Militzer, Fateh Fazeli and Hamid Azizi-Alizamini
The Centre for Metallurgical Process Engineering,
The University of British Columbia
Vancouver, BC, Canada V6T 1Z4

Paper presented at the 2nd International Conference on Super High Strength Steels, Peschiera del Garda, 16-20 October 2010, organized by AIM

AUSTENITE DECOMPOSITION DURING RUN-OUT TABLE COOLING

Phenomenological models have been developed for the austenite-to-ferrite and pearlite transformations during run-out table cooling of low carbon steels including microalloyed grades [6, 9] with conventional ferrite-pearlite microstructures. A sequential transformation model has been proposed that consists of sub-models for ferrite start, ferrite growth, pearlite start and pearlite growth [9, 14]. The models are based on the Johnson-Mehl-Avrami-Kolmogorov (JMAK) approach incorporating additivity. More recently, when considering the extension of these models to dual-phase (DP), transformation-induced plasticity (TRIP) and complex-phase (CP) steels the sequential transformation model has been extended to include the bainite and martensite transformations [15, 16, 17, 18, 19]. In most of these advanced high strength steels it is sought to minimize the formation of pearlite by suitable alloying strategies. Then, the transformation model for these steels can be formulated using the following five sub-models: (i) ferrite start, (ii) ferrite growth, (iii) bainite start, (iv) bainite growth, and (v) martensite start. To tailor the phase transformations in these steels a number of alloying elements are added, e.g. Nb, Mo, B, that when remaining in solution are extremely effective in delaying austenite decomposition. Thus, it is critical to explicitly include the role of solutes into the transformation models.

For low carbon steels, Militzer et al. [9,20] proposed a ferrite transformation start model for run-out table cooling. The transformation start temperature is predicted by assuming that carbon diffusion controlled early growth of ferrite nucleated at temperature, T_N, at grain corners determines nucleation site saturation at austenite grain boundaries. Adopting spherical geometry and steady state diffusional growth, the radius, R_f, of the corner nucleated ferrite can be calculated from

$$\frac{dR_f}{dT}\frac{dT}{dt} = D_C \frac{c_\gamma - c_0}{c_\gamma - c_\alpha}\frac{1}{R_f} \quad (1)$$

where D_C is the diffusivity of carbon in austenite, c_0 is the average carbon concentration and c_α and c_γ are the carbon equilibrium concentrations in ferrite and austenite, respectively. Measurable transformation start (i.e. 5% transformed) is assumed to coincide with nucleation site saturation at prior austenite grain boundaries which is reached when carbon enrichment at the austenite boundaries attains a critical level, c*, above which ferrite nucleation is inhibited, i.e.

$$R_f \geq \frac{c^* - c_0}{c_\gamma - c_0}\frac{d_{\gamma eff}}{\sqrt{2}} \quad (2)$$

where the effective austenite grain size is given by [21]

$$d_{\gamma eff} = d_\gamma \exp(-\varepsilon_r) \quad (3)$$

to account for the degree of pancaking due to incomplete recrystallization in the finishing mill. Here, d_γ is the austenite grain size and ε_r is the strain applied under no-recrystallization conditions. The above approach does not explicitly deal with the role of alloying elements in solution. In particular, Nb in solution is very effective in delaying the onset of ferrite formation. Thus, dedicated laboratory studies were conducted to quantify the transformation behaviour in a Nb-Ti microalloyed linepipe steel (0.06C-1.65Mn-0.034Nb-0.012Ti-0.24Mo (wt pct)) with Nb in solution and Nb precipitated. For this purpose, dilatometric transformation studies were conducted using a Gleeble 3500 thermo-mechanical simulator as described elsewhere in more detail [20]. To control the amount of Nb in solution and limit austenite grain growth specific heat treatment cycles were conducted prior to austenite decomposition. To keep Nb in solution samples were solution treated by heating at 10 °C/s to 1300 °C and holding there for 35 s before cooling at 100 °C/s to ambient temperature. Then, the samples were immediately reheated at 1000 °C /s to a desired austenitizing temperature resulting in austenite grain sizes of 5 μm and 40 μm (mean equivalent area diameter), respectively, before executing continuous cooling transformation (CCT) tests at a prescribed cooling rate, Ψ. In contrast, following the single stage reheating to an austenitizing temperature, re-precipitation of Nb was accomplished by holding for 20 min at 900 °C before commencing the CCT tests. The holding at 900 °C does not affect the austenite grain size. Based on the experimental results, an extension of the ferrite transformation start model is proposed by incorporating a solute drag term into equation (1), i.e.

$$\frac{dR_f}{dT}\frac{dT}{dt} = D_C \frac{c_\gamma - c_0}{c_\gamma - c_\alpha}\frac{1}{R_f}\left(1 + \frac{D_C \alpha C_{sol}}{R_f}\right)^{-1} \quad (4)$$

where C_{sol} is the amount of Nb in solution in weight percent and α is a solute drag parameter. As illustrated in Figure 1, this model extension enables to describe the effect of Nb in solution on the ferrite transformation start in the investigated linepipe steel. The transformation start is here quantified as undercooling below the Ae_3 temperature (820 °C for the linepipe steel). The fit parameters for this steel have been determined to be T_N = 700 °C, c^*/c_0=2.3 and α= 800 s $\mu m^{-1}(wt\%)^{-1}$. Nb in solution can delay the onset of ferrite formation for accelerated cooling conditions (>10 °C/s) by approximately 100 °C. This observation is similar to those reported in the literature for other Nb steels [22].

Subsequent ferrite growth can be described with the JMAK approach adopting additivity, i.e.

$$X = 1 - \exp\left\{-\left(\int_{T_s}^{T} \frac{b(T)^{1/k}}{\Psi(T)}dT\right)^k\right\} \quad (5)$$

where the normalized ferrite fraction, X, represents the actual ferrite fraction in units of the equilibrium ferrite fraction, Ψ=dT/dt is the instantaneous cooling rate and T_s is the transformation start temperature. The JMAK exponent k can usually be approximated with k=1 for the ferrite transformation and the rate function b depends on prior austenite grain size and temperature such that

$$b = \frac{b_\alpha}{d_\gamma^m} \quad (6)$$

where m is the grain size exponent and b_α is a temperature dependent rate function [23]. Both parameters are a function of steel chemistry. Further, for better descriptive capabilities, b_α is in selected cases expressed as a function of the carbon content in remaining austenite, $c_{\gamma\text{-rem}}$, that increases with the fraction transformed. The JMAK approach fulfills the additivity principle as long as $\ln b_\alpha$ is in the form of $\ln b_\alpha = y(T) + z(X)$ where y and z are functions of T and X, respectively [24]. As a general rule, three parameters are needed to establish b_α for ferrite formation during run-out table cooling of a given steel such that together with m there are in total four adjustable parameters.

From a more fundamental perspective a mixed-mode approach can be adopted [25]. Here, long range carbon diffusion and the interface reaction are both considered and this has been shown to be appropriate for low carbon steels [25,26,27]. There are a couple of challenges with this approach. It is still a matter of debate whether paraequilibrium or negligible-partition local equilibrium provides the suitable condition in the limit of a long range carbon diffusion controlled reaction [28]. Further, the interface mobility has to be determined as an effective parameter by fitting to experimental data. Fazeli and Militzer [27] proposed an effective mobility that incorporates a solute drag model such that all parameters are well defined in their physics. Neverthe-

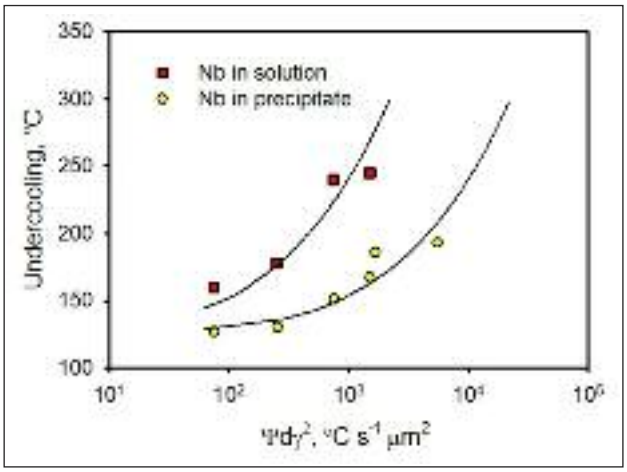

FIG. 1 ***Transformation start in the linepipe steel with Nb precipitated and in solution.***

Inizio della transformazione in un acciaio da tubazioni con Nb precipitato e in soluzione.

less, this approach requires to determine four of these parameters from experimental transformation data, i.e. a similar number of fit parameters as in the more conventional JMAK approach. To further improve the predictive capability of the JMAK approach, the solute drag effect of alloying elements can be included in a pragmatic fashion. This is particularly relevant for Nb containing steels and the methodology resembles that presented above for the modification of the ferrite start model (cf. eq. 4). However, the more physically based approach promises to provide a more reliable insight into the role of individual alloying elements on ferrite growth.

The bainite start temperature, B_s, can be comparatively easily quantified in Mo containing steels where ferrite and bainite reactions are usually clearly separated [19,29]. For sufficient Mo addition ferrite stasis has been observed [30]. Using CCT data for Mo-containing steels, i.e. a TRIP chemistry (0.19C-1.5Mn-1.6Si-0.2Mo (wt pct)) and a CP chemistry (0.05C-1.88Mn-0.49Mo-0.048Nb (wt pct)), B_s can be described with the concept of a critical driving pressure, G_{crit}, originally proposed by Ali and Bhadeshia [31]. For these two steels the following relationship has been found

$$G_{crit}(\text{Jmol}) = -4.55T(°C) + 3423 \quad (7)$$

independent of steel chemistry, as illustrated in Figure 2. Studies on other steels that do not contain Mo suggest that a similar critical driving pressure concept can be applied, as illustrated in Figure 2 with data of estimated bainite start temperatures in a Nb microalloyed steel (0.06C-1.5Mn-0.2Si-0.047Nb (wt pct)). However, it is a challenge to clearly determine the onset of bainite formation in these steels with a more gradual transition from polygonal to bainitic ferrite. Further, a clear separation of these two constituents in the final microstructure with a frequently acicular appearance may involve significant inaccuracies.

In a first approximation, bainite growth can, similar to ferrite growth, be described with the JMAK model. However, the bainite reaction is in general non-additive such that there are significant limitations for the applicability of this approach. As proposed by Tao et al. [24], a bainite modelling strategy can be employed where the JMAK parameters are just applicable to the initial fine-grained austenite or austenite-ferrite microstructures encountered in hot strip mills and associated cooling scenarios that indeed lead to a significant portion of bainitic ferrite in the final microstructure, i.e. 30% and higher. Clearly, further work is required to establish robust models for the bainite formation with predictive capabilities for a wide range of industrial processing conditions.

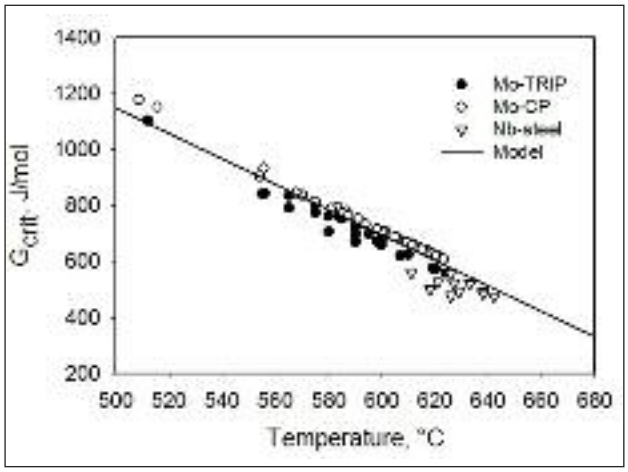

FIG. 2 ***Bainite start in low carbon steels.***

Inizio della trasformazione bainitica negli acciai a basso carbonio.

The cessation of the bainite transformation stage is currently predicted from empirical relationships that have been proposed for the martensite start temperature [32]. It is critical to use the chemical composition of the remaining austenite when employing these relations, i.e. carbon enrichment has to be taken into account. However, these relationships need to be critically reviewed as other microstructure aspects, for example the size of remaining austenite islands, determine their stability [33]. In case of steels without a significant bainite portion, e.g. ferrite-martensite DP steels, the problematic of describing the bainite transformation can be circumferenced by considering the average cooling rate between an estimated ferrite stop temperature, e.g. 600 °C, and the martensite start temperature [18]. Above a critical cooling rate, all remaining austenite is assumed to transform to martensite.

AUSTENITE FORMATION DURING INTERCRITICAL ANNEALING

For automotive applications, frequently intercritical annealing of cold-rolled sheets is the crucial processing step to generate the required multi-phase microstructures of advanced high strength steels. During intercritical annealing an austenite-ferrite microstructure forms where fraction, size and distribution of austenite set the stage for the martensite and/or bainite reactions during subsequent cooling and annealing steps. As illustrated in Figure 3 for a DP 600 chemistry (0.10C-1.86Mn-0.16Si-0.34Cr (wt pct)), partial austenite formation during intercritical annealing leads to morphologically complex austenite aggregates. Figure 3a shows an example of the resulting microstructure when the 50% cold-rolled steel is continuously heated at 1 °C/s to 790 °C before quenching whereas Figure 3b depicts the situation where the steel is heated at 10 °C /s to 780 °C before quenching. The martensite distribution that results from the quench reflects the intercritical austenite. Clearly, the austenite distribution is morphologically complex and vastly different in both heating scenarios. At the lower heating rate, ferrite recrystallization is completed before the onset of austenite formation such that a necklace-type austenite microstructure forms with a number of finger-like features. For the higher heating rate, on the other hand, ferrite recrystallization is not yet completed before austenite formation. As a result, a more banded austenite microstructure forms that also displays some of the finger-like features.

To capture the morphological complexity of this transformation, modelling on the meso-scale is appropriate using the phase field approach. The status of austenite formation models are illustrated with 2D phase field simulations for plain carbon steels. As described elsewhere in more detail [34], microstructure simulations were conducted with a multi-phase field approach using the commercially available code MICRESS (microstructure evolution simulation software) [35]. The formulation of this phase field approach is based on the work of Steinbach et al. [36]. Here, each grain i is prescribed by its own phase field parameter ϕ_i [i=1,...,N] where ϕ_i is equal to 1 inside grain i and 0 elsewhere. At the interface between two grains there is a gradual change of the two corresponding phase field parameters from 0 to 1 such that

$$\sum_{i}^{N} \phi_i(r,t) = 1$$

holds at each position, r, in the simulation domain with a total

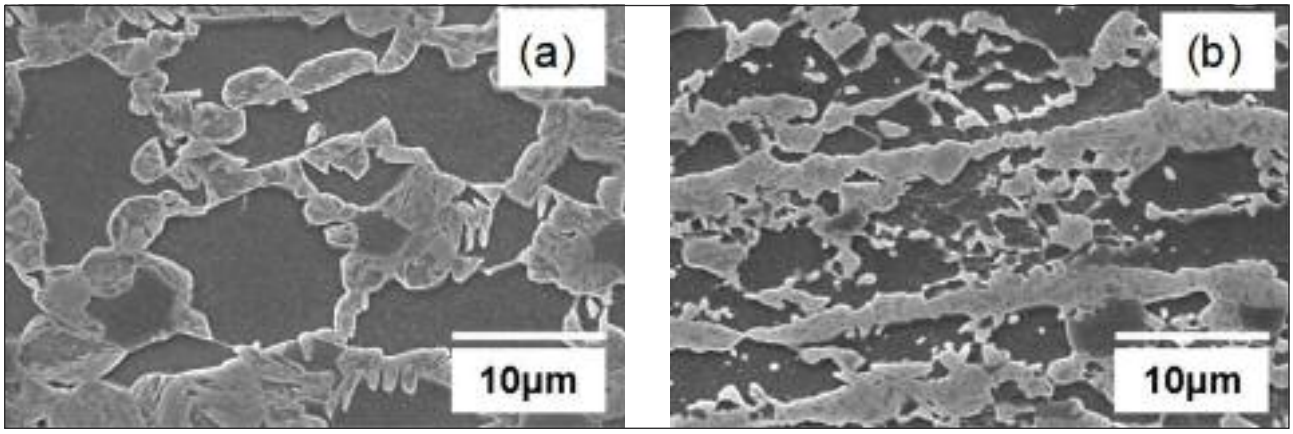

FIG. 3 ***Intercritical austenite in the DP600 steel: (a) heating at 1 °C /s to 790 °C, (b) heating at 10 °C /s to 780 °C.***
Austenite intercritica nell'acciaio DP600: (a) riscaldamento di 1 °C /s fino a 790 °C, (b) riscaldamento di 10 °C /s fino a 780 °C.

number of N grains. The rate of change of the phase field parameters is given by a set of coupled differential equations [36]:

$$\frac{d\phi_i}{dt} = \sum_{j \neq i} \mu_{ij} \left[\sigma_{ij} \left\{ \phi_j \nabla^2 \phi_i - \phi_i \nabla^2 \phi_j + \frac{\pi^2}{2\eta_{ij}^2} (\phi_i - \phi_j) \right\} + \frac{\pi}{\eta_{ij}} \sqrt{\phi_i \phi_j} \Delta G_{ij} \right] \quad (8)$$

where μ_{ij} is the interface mobility, σ_{ij} is the interfacial energy, η_{ij} is the interface thickness and ΔG_{ij} is the driving pressure. The evolution of the phase field parameters describing the microstructure is governed by minimization of the total free energy of the system. The phase field equations are coupled with the diffusion equations for carbon to describe phase transformations in the Fe-C system [37]. Then, the model is consistent with the mixed-mode approach that is relevant for the austenite-ferrite transformation in low carbon steels. The degree of the mixed-mode character of the transformation depends on the interface mobility. Taking a sufficiently large mobility, the transformation is carbon diffusion controlled.

For the diffusion controlled regime, 2D simulations of austenite formation have been conducted for isothermal holding at 750 °C of an Fe-0.17C (wt pct) alloy with a ferrite-pearlite initial structure. The set up of the calculation domain and selection of parameters (μ_{ij}, σ_{ij}, η_{ij}, ΔG_{ij}) followed the approach described in a previous paper [34] where austenite formation from ferrite with spherical cementite particles had been considered. In the present calculations, however, a much finer grid size of 5 nm had to be employed to resolve the fine cementite lamellae and having a ferrite-cementite interface width of four grid points. Figure 4 provides a sequence of the simulated microstructure evolution where ferrite is shown in red, cementite in yellow and austenite in white. Austenite nuclei have been assumed to form at the intersection of ferrite with pearlite colonies (Fig. 4a). The austenite is predicted to grow preferentially along the cementite lamellae (Fig. 4b). Due to growth perpendicular to the cementite lamellae different austenite grains impinge and a typical finger-type morphology of austenite results (Fig. 4c). Complete dissolution of cementite is slower than the progression of the austenite front through the pearlite colony such that temporarily some cementite is retained within austenite (Figs. 4b, 4c). Overall growth of austenite into pearlite is much faster than its growth into ferrite that is required to reach the equilibrium austenite fraction (Fig. 4d). These simulation results replicate qualitatively experimental observations. The formation of finger-type morphologies is typical for austenite formation [38], as also observed in the micrographs shown in Fig. 3. Further, the rapid pearlite-to-austenite transformation has been confirmed experimentally [38,39]. Both of these aspects are related to the fact that the supply of carbon is a rate-limiting factor for austenite formation, i.e. austenite grows preferentially towards carbides as the sources of carbon.

These phase field simulations for the Fe-C system realistically describe important qualitative and quantitative aspects of austenite formation. However, to do similar simulations for advanced high strength steels it will be required to account for the role of substitutional alloying elements, e.g. Mn, Si, Mo. From a pragmatic point of view, an effective mobility approach may be taken where the interface mobility of austenite with its parent phases (ferrite, cementite) is adjusted to replicate experimentally observed austenite formation rates. The concept of an effective interface mobility is illustrated below for austenite grain growth.

AUSTENITE GRAIN GROWTH IN THE HAZ

During girth welding the control of the microstructure in the HAZ is of paramount importance. In particular control of austenite grain growth is crucial as it provides the initial structure for the subsequent austenite decomposition. In particular, excessively large austenite grains near the fusion line are of concern as they may lead to martensitic and/or bainitic transformation products with adverse effects on properties, e.g. decreased fracture toughness [40]. The HAZ experiences rapid thermal cycles and steep temperature gradients. As a result, meso-scale modelling, here phase field modelling, is not only an appropriate but necessary tool to account for thermal pinning due to steep temperature gradients.

As for austenite formation, MICRESS has been used in conjunction with an effective mobility approach, i.e. the set of differential equations given by eq. (8) are employed where for grain growth $\Delta G_{ij} = 0$. The effective mobility of the austenite grain boundaries has been determined from experimental grain growth studies by Banerjee et al. [41] for rapid continuous heating of bulk samples of the linepipe grade (0.06C-1.65Mn-0.034Nb-0.012Ti-0.24Mo (wt pct)) previously introduced for the transformation studies with Nb in solution and precipitated. Based on the experimental results, Banerjee et al. [41] proposed a phenomenological model to correlate austenite grain growth with dissolution of NbCN, i.e. a reduction in particle pinning pressure. Alternatively, an effective grain boundary mobility can be introduced to replicate grain growth for the rapid heat treatment cycles in the HAZ with time and temperature dependent particle pinning pressure [42]. These effective mobilities are

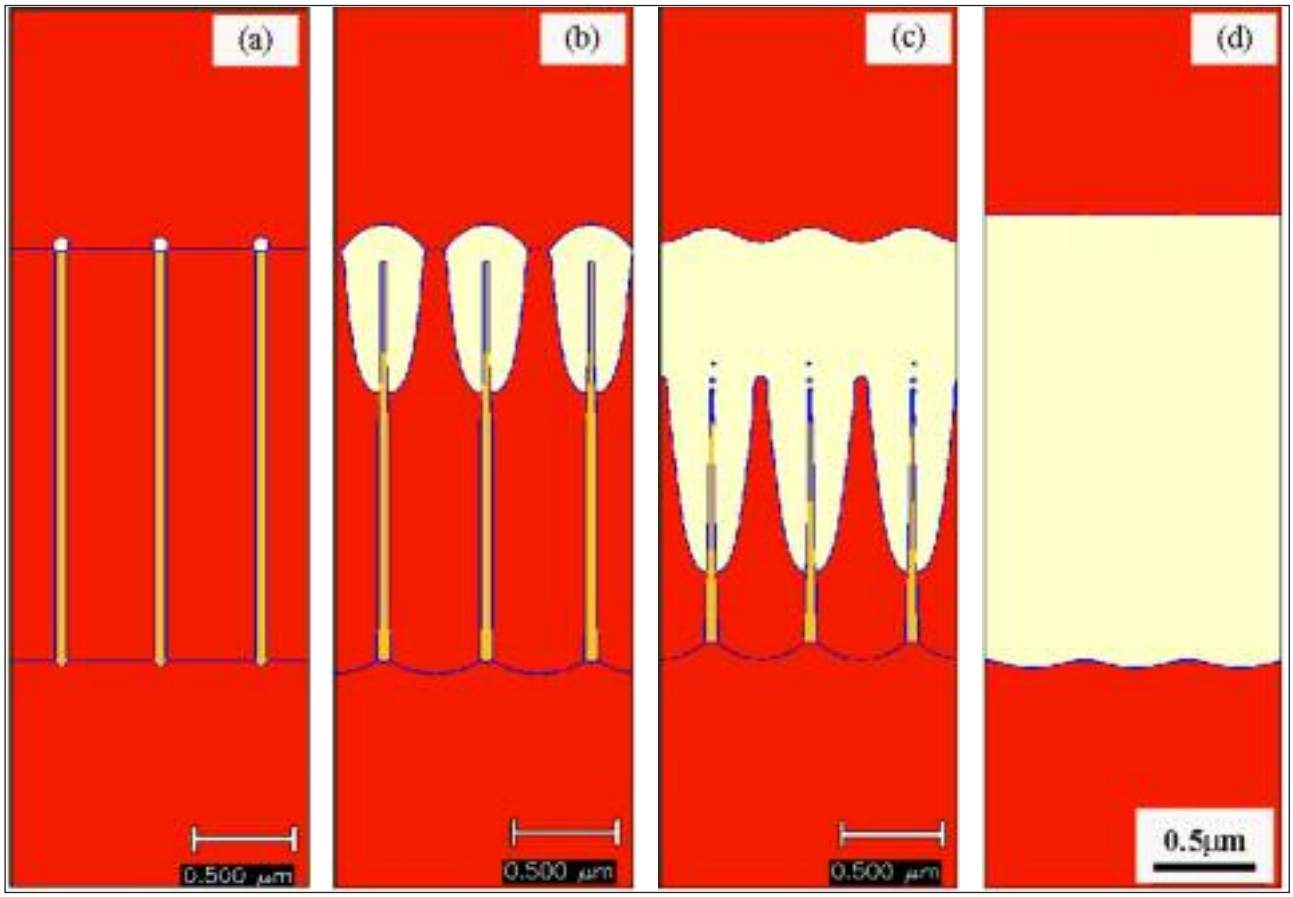

FIG. 4 ***Phase field simulation of austenite formation in an Fe-0.17 C (wt pct) steel at an intercritical annealing temperature of 750°C, (a) initial ferrite-pearlite structure with austenite nuclei, (b) 0.05s, (c) 0.1s, (d) 0.25s.***

Simulazione del campo di fase della formazione di austenite in un acciaio Fe-0.17 C (% in peso) alla temperatura di trattamento intercritico di 750°C, (a) struttura iniziale ferrite-perlite con nuclei di austenite, (b) dopo 0.05s, (c) dopo 0.1s, (d) dopo 0.25s.

consistent with a low mobility branch for strong pinning at lower temperatures and a high mobility branch for weak pinning at higher temperatures separated by the estimated dissolution temperature range of fine NbCN precipitates.

Using these mobility parameters, two and three dimensional (2D/3D) phase field simulations were conducted assuming periodic boundary conditions. In a first set of simulations, the proposed approach was tested for continuous heating and cooling conditions in bulk samples without thermal gradients but subjected to thermal cycles that are typical for various positions in the HAZ. Figure 5 compares grain structures obtained in phase field simulations with those observed experimentally for heating at 1000 °C/s to 1350 °C and cooling at 100 °C/s to 900 °C with a residence time of 0.5 s at the peak temperature. The selected peak temperature is above the dissolution temperature of NbCN such that a situation is depicted where substantial grain growth can take place. As can be seen in Figure 5, simulated and experimental grain structures are in excellent agreement – an observation that was also verified for other heating paths [42]. Both 2D and 3D simulations give the same grain size when using an effective mobility in 3D that is by a factor of 0.7 smaller than the effective mobility in 2D [43]. The effective mobility approach is appropriate for the short heat treatment cycles of the HAZ but if longer heat treatments were considered a pinning term would have to be explicitly introduced to obtain a limiting grain size that results from particle pinning.

After having validated the proposed model with austenite grain growth in bulk samples, the model has been applied to predict grain growth in the HAZ. Here, in the direction perpendicular to the fusion line, i.e. for the domain boundary plane parallel to the fusion zone, periodic boundary conditions are replaced by insulating boundary conditions. Further, thermal profiles have to be established as a function of distance from the fusion line. During welding trials for the investigated linepipe steel thermal cycles were measured with thermocouples at selected positions in the HAZ. The temperature data obtained in the welding trials were fitted to a general form of the Rosenthal equation that was taken as model input for the time-temperature paths. To limit computational cost, grain growth was simulated in 2D for a horizontal section of the HAZ. Further, the HAZ was sub-divided into nine sub-domains with time dependent linear thermal gradients with the Rosenthal fit providing the time-temperature path at the positions of the domain boundaries parallel to the fusion line. Figure 6 shows the simulated austenite grain structure in the HAZ confirming a gradual decrease of grain size with increasing distance from the fusion zone. The region close to the fusion zone is of particular interest where the coarsest austenite grains form. In the welding trials this region (up to 200 µm from the fusion line) displays a bainitic microstructure that permits, at least to a first approximation, to estimate prior austenite grain sizes. For this region the average grain size was found to be 30 µm and a maximum size of 55 µm was observed while the 2D phase field simulations predict an average grain size of 20 µm and a maximum size of 35 µm. Even though 2D simulations provide promising results for the HAZ, 3D simulations are expected to be of increased relevance when modelling grain growth in the

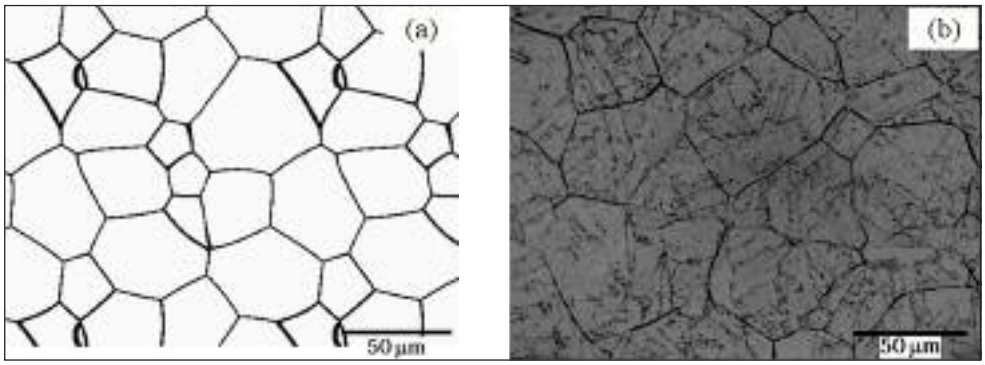

FIG. 5
Non-isothermal austenite grain growth in the linepipe steel heated at 1000 °C/s to 1350 °C and cooled at 100 °C/s to 900 °C: (a) representative 2D cut of 3D phase field simulation, (b) experimental observation of Banerjee et al. [41].

Crescita non-isotermica del grano austenitico nell'acciaio da tubazioni riscaldato a 1000 °C/s fino a 1350 °C e raffreddato a 100 °C/s fino a 900 °C: (a) rappresentazione in sezione 2D della simulazione 3D del campo di fase, (b) osservazione sperimentale di Banerjee et al. [41].

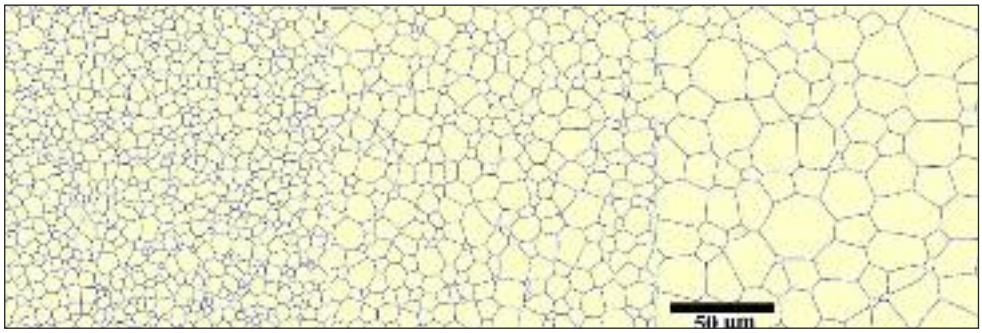

FIG. 6
2D phase field simulation of austenite grain growth in the HAZ of the linepipe steel.

Simulazione 2D del campo di fase della crescita del grano di austenite nell' HAZ di un acciaio per tubazioni.

HAZ with steep temperature gradients where grain growth may be affected by thermal pinning. Closer examination of Figure 6 indicates a number of boundary lines close to the fusion zone that are straight in 2D but in 3D these boundaries would still have a curvature in the plane perpendicular to the 2D calculation plane and this may markedly affect the actual grain growth behaviour and resulting grain morphology.

CONCLUSIONS

Significant progress has recently been made in developing microstructure evolution models for state-of-the-art advanced high strength steels by extending model concepts that previously had been proposed for conventional steels with ferrite-pearlite microstructures. However, these established approaches that frequently are based on the classical JMAK theory have a number of limitations that become increasingly apparent when considering the predictive capabilities for complex microstructure events, e.g. bainite transformation and austenite formation.

Modelling on the meso-scale using phase field models is a promising tool when morphological complexities are significant as illustrated for austenite formation or when considering microstructure evolution under the presence of a steep temperature gradient as shown for the HAZ. Nevertheless, phase field models are descriptive in nature and require input parameters that have to be obtained from experimental studies. For a given process, it is frequently possible to make pragmatic simplifications of the models, e.g. by employing effective interface mobilities.

To propose next generation microstructure process models with improved predictive capabilities it is necessary to increasingly replace semi-empirical and/or pragmatic concepts with sound physical approaches where all parameters and their underlying physics are clearly defined. In particular the role of substitutional alloying elements and their interaction with moving grain boundaries and interfaces is a critical aspect in achieving the goal of having predictive microstructure models. A combination of state-of-the-art experimental studies, e.g. atom probe, and theoretical investigations using a multi-scale modelling approach is suggested to push the frontiers of the envisioned model development. In the computational approach it is critical to explore the capabilities of atomistic simulations, i.e. ab-initio density functional theory and classical molecular dynamics, to provide information and guidance on mobility and solute drag parameters that are currently challenging to measure directly from experimental investigations.

ACKNOWLEDGEMENT

The financial support received from the Natural Sciences and Engineering Research Council of Canada, ArcelorMittal Dofasco Inc., Essar Steel Algoma, Evraz Inc. NA and TransCanada Pipelines is acknowledged with gratitude. The authors would like to thank S. Sarkar, D. Liu, S. Gerami, R. Tafteh, M. Toloui, M. Kulakov and J. Tao for their critical contributions to the presented work.

REFERENCES

1) C. M. SELLARS and J. A WHITEMAN, Met. Sci. 13, (1979), p. 187.
2) C. M. SELLARS, Sheffield Int. Conf. on Working and Forming Processes, Sheffield (1980), Met. Soc., London, UK, p. 3.
3) A. YOSHIE, M. FUJIOKA, Y. WATANABE, K. NISHIOKA and H. MORIKAWA, ISIJ Int. 32, (1992), p. 395.
4) Y. SAITO and C. SHIGA, ISIJ Int. 32, (1992), p. 414.
5) J. ANDORFER, D. AUZINGER, B. BUCHMAYR, W. GISELBRECHT, G. HRIBERNIG, G. HUBMER, A. LUGER and A. SAMOILOV, Thermec'97, Wollongong (1997), TMS, Warrendale, PA, p. 2069.
6) M. SUEHIRO, K. SATO, Y. TSUKANO, H. YADA, T. SENUMA and Y. MATSUMURA, Trans. ISIJ 27, (1987), p. 439.
7) R. SHULKOLSKY, D. L. ROSBURG, J. D. CHAPMAN and K. R. BARNES, Modeling, Control and Optimization in Nonferrous and Ferrous Industries, Chicago (2003), TMS, Warrendale, PA, p. 509.
8) A. PERLADE, D. GRANDEMANGE and T. IUNG, Ironmaking Steelmaking 32 (2005), p. 299.
9) M. MILITZER, E. B. HAWBOLT and T. R. MEADOWCROFT, Metall. Mater. Trans. 31A, (2000), p. 1247.
10) L. KESTENS and J.J. JONAS, ISIJ Int. 37, (1997), p. 807.
11) M. PIETRZYK, C. ROUCOULES and P.D. HODGSON, ISIJ Int. 35,

(1995), p. 531.
12) T. IUNG, M. AZUMA, O. BOUAZIZ, M. GOUNE, A. PERLADE and D. QUIDORT, Mater. Sci. Forum 426-432, (2003), p. 3849.
13) J.B. LEBLOND and J.C. DEVAUX, Acta Mater. 32, (1984), p. 137.
14) M. MILITZER, R. PANDI, E.B. HAWBOLT and T.R. MEADOWCROFT, Hot Workability of Steels and Light Alloys-Composites, Montreal (1996), The Metallurgical Society of CIM, Montreal, PQ, p. 373.
15) A. SAMOILOV, Y. TITOVETS, N. ZOLOTOREVSKII, G. HRIBERNIG and P. STIASZNY, Proc. 2nd Int. Conf. Processing Materials for Properties, San Francisco (2000) TMS, Warrendale, PA, p. 639.
16) H.N. HAN and S.H. PARK, Mater. Sci. Technol. 17, (2001), p. 721.
17) D. LIU, F. FAZELI, M. MILITZER and W.J. POOLE, Metall. Mater. Trans. 38A, (2007), p. 894.
18) D. LIU, F. FAZELI and M. MILITZER, ISIJ Int. 47, (2007), p. 1789.
19) S. SARKAR and M. MILITZER, Mater. Sci. Technol. 25, (2009), p. 1134.
20) M. MILITZER, R. PANDI and E. B. HAWBOLT, Metall. Mater. Trans. 27A, (1996), p. 1547.
21) S. LACROIX, Y. BRÉCHET, M. VERON, D. QUIDORT, M. KANDEL and T. IUNG, Austenite Formation and Decomposition, Chicago (2003), TMS, Warrendale, PA, p. 367.
22) L.E. COLLINS and W.J. LIU, Phase Transformations During the Thermal/Mechanical Processing of Steel, Vancouver (1995), The Metallurgical Society of CIM, Montreal, PQ, p. 419.
23) I. TAMURA, H. SEKINE, T. TANAKA and C. OUCHI, Thermomechanical Processing of High Strength Low Alloy Steels. Butterworth and Co., London, UK (1988), p. 21.
24) J. TAO, M. MILITZER and Z.Y. LIU, ISIJ Int. 50, (2010), p. 583.
25) G. P. KRIELAART, J. SIETSMA and S. VAN DER ZWAAG, Mat. Sci. Eng. A327, (1997), p. 216.
26) J. SIETSMA and S. VAN DER ZWAAG, Acta Mater. 52, (2004), p. 4143.
27) F. FAZELI and M. MILITZER, Metall. Mater. Trans. 36A, (2005), p. 1395.
28) H.S. ZUROB, C.R. HUTCHINSON, A. BECHE, G. PURDY and Y. BRÉCHET, Acta Mater. 56, (2008), p. 2203.
29) F. FAZELI and M. MILITZER, Mater. Sci. Forum 539-543, (2007), p. 4339.
30) H.I. AARONSON, W.T. REYNOLDS and G.R. PURDY, Metall. Mater. Trans. 37A, (2006), p. 1731.
31) A. ALI and H.K.D.H. BHADESHIA, Mat. Sci. Tech. 5, (1989), p. 398.
32) W. STEVEN and A.G. HAYNES, JISI 183, (1956), p. 349.
33) E. JIMENEZ-MELERO, N.H. VAN DIJK, L. ZHAO, J. SIETSMA, S.E. OFFERMAN, J.P. WRIGHT and S. VAN DER ZWAAG, Acta Mater. 55, (2007), p. 6713.
34) H. AZIZI-ALIZAMINI and M. MILITZER, Int. J. Mat. Res. 101, (2010), p. 534.
35) http://www.access.rwth-aachen.de/MICRESS/
36) I. STEINBACH, F. PEZZOLLA, B. NESTLER, M. SEEßELBERG, R. PRIELER, G.J. SCHMITZ and J.L.L. REZENDE, Phys. D 94, (1996), p. 135.
37) M.G. MECOZZI, J. SIETSMA, S. VAN DER ZWAAG, M. APEL, P. SCHAFFNIT and I. STEINBACH, Metall. Mater. Trans. 36A, (2005), p. 2327.
38) V.I. SAVRAN, Y. VAN LEEUWEN, D.N. HANLON, C. KWAKERNAAK, W.G. SLOOF and J. SIETSMA, Metall. Mater. Trans. 38A, (2007), p. 946.
39) G.R. SPEICH, V.A. DEMAREST and R.L. MILLER, Metall. Trans. 12A, (1981), p. 1419.
40) F. HAMAD, L. COLLINS and R. VOLKERS, Proc. 7th Internat. Pipeline Conf. (IPC2008), Calgary (2008), ASME, IPC2008, p. 553.
41) K. BANERJEE, M. MILITZER, M. PEREZ and X. WANG, Metall. Mat. Trans. A, 41A, (2010), p. 3161.
42) M. TOLOUI and M. MILITZER, Int. J. Mat. Res. 101, (2010), p. 542.
43) M. TOLOUI and M. MILITZER, Proc. Recrystallization and Grain Growth IV, Sheffield (2010), in press.

Abstract

Modellazione dell'evoluzione microstrutturale negli acciai avanzati ad alta resistenza

Parole chiave: acciaio, modellazione

Negli ultimi anni si è assistito ad un significativo sviluppo di nuove famiglie di acciai – come ad esempio gli acciai avanzati ad alta resistenza - in risposta alle crescenti esigenze delle industrie automobilistiche e nel settore delle costruzioni che richiedono materiali con caratteristiche migliorate. La trasformazione austenite-ferrite è lo strumento metallurgico principale per determinare le caratteristiche degli acciai. Lo sviluppo di nuovi processi in grado di portare alle microstrutture desiderate è stato sempre più supportato dalla simulazione al computer. Il presente lavoro illustra lo stato dell'arte della modellazione delle microstrutture per gli acciai a basso carbonio prendendo in considerazione tre aspetti importanti del processo: (i) tavolo di raffreddamento run-out degli acciai laminati a caldo, (ii) riscaldamento intercritico di fogli laminati a freddo, (iii) saldatura circonferenziale di acciai per tubazioni. Modelli fenomenologici basati sull' approccio Johnson Mehl-Avrami-Kolmogorov (JMAK), che incorporano l'additività sono oggi disponibili per descrivere trasformazioni di fase durante il raffreddamento su nastro degli acciai microlegati. Nel presente lavoro saranno discussi i punti di forza e i limiti di questo approccio. I modelli per il processo di ricottura intercritica richiedono una descrizione accurata della cinetica di formazione dell'austenite dove le complessità morfologiche possono essere colte usando l'approccio del campo di fase. Durante la saldatura circonferenziale il controllo della microstruttura nella zona termicamente alterata (ZTA) è di importanza primaria. La zona HAZ viene sottoposta a rapidi cicli termici e rapidi gradienti di temperatura. La modellazione del campo di fase risulta essere un ottimo strumento per descrivere il ruolo di questi vincoli spaziali, come verrà illustrato per la crescita del grano austenitico.